

Human Activity Recognition Using Self-Supervised Representations of Wearable Data

Maximilien Burq *
Verily Life Sciences
mburq@verily.com

Niranjana Sridhar *
Verily Life Sciences
nirsd@verily.com

Abstract

Automated and accurate human activity recognition (HAR) using body-worn sensors enables practical and cost efficient remote monitoring of Activity of Daily Living (ADL), which are shown to provide clinical insights across multiple therapeutic areas. Development of accurate algorithms for human activity recognition (HAR) is hindered by the lack of large real-world labeled datasets. Furthermore, algorithms seldom work beyond the specific sensor on which they are prototyped, prompting debate about whether accelerometer-based HAR is even possible [Tong et al., 2020] .

Here we develop a 6-class HAR model with strong performance when evaluated on real-world datasets not seen during training. Our model is based on a frozen self-supervised representation learned on a large unlabeled dataset, combined with a shallow multi-layer perceptron with temporal smoothing. The model obtains in-dataset state-of-the-art performance on the Capture24 dataset ($\kappa = 0.86$). Out-of-distribution (OOD) performance is $\kappa = 0.7$, with both the representation and the perceptron models being trained on data from a different sensor.

This work represents a key step towards device-agnostic HAR models, which can help contribute to increased standardization of model evaluation in the HAR field.

1 Introduction

Assessments of activities of daily living (ADL) are used in the early detection, diagnosis, treatment, and care of many health conditions, including arthritis, depression, stroke, heart failure, Parkinson’s disease, dementia, and Alzheimer’s disease [Marshall et al., 2012, Clynes et al., 2019, Kazama et al., 2011, Lawrence et al., 2014, Fauth et al., 2013, Sandberg et al., 2001, Williamson et al., 2021, Wainberg et al., 2021, Lam et al., 2021]. Numerous clinical diagnostic tests [authors listed, 2003, Kroenke et al., 2001, de Rotrou et al., 2012] include ADL assessments, typically using self-reported data. While such data provide valuable perspectives, complementing them with objective measures can enable comparison of symptoms and outcomes over time or across different patients and allow the effects of interventions to be quantified. Recent advances in wearable technology have enabled the large scale deployment of sensors and algorithms for human activity recognition (HAR). Such measures allow consumers to track their health metrics over time and are emerging as valuable digital biomarkers in clinical studies [Marra et al., 2020].

*Equal contributions

1.1 Related work

Attempts to develop HAR models on smartwatches, smartphones, other body-worn sensors, or via radar, video, and other ambient sensors, have been hampered by a lack of large datasets - ones with high-quality reference activity labels in real-life settings - that can be used to build and test models. For real-world data collection, obtaining high-quality labels of human activities alongside the sensor data stream requires manual annotation of video-based ground-truth, which is costly and can be intrusive for the participants. Alternatively, participants can self-report their activities, but this introduces variability and noise due to participant subjectivity, as well as a selection bias of the activities they choose to report.

1.2 Supervised HAR models

Due to these obstacles, most HAR benchmark datasets [Reiss and Stricker, 2012, Banos et al., 2015, Bruno et al., 2013, Altun et al., 2010, Malekzadeh et al., 2018, Zhang and Sawchuk, 2012] contain data on fewer than 20 research participants, performing 1 to 15 activities for up to 5 minutes under constrained or clinic-like conditions. Given the small size and low ecological validity of these datasets, models trained and tested on them may fail to generalize to the real world when faced with activities not previously encountered, or when applied to new devices or sensors. Furthermore, due to the small size of the datasets available, researchers typically rely on extensive manual feature engineering, which can lead to overfitting when evaluation is through cross-validation without an explicit test dataset.

While some published studies report near 100% accuracy on these datasets individually, cross-dataset performance has not approached such levels of accuracy, prompting debate about whether accelerometer-based HAR is even possible [Tong et al., 2020]. The generalization problem strongly constrains the utility of supervised HAR models in practical applications. HAR models trained on small datasets of curated activity labels can only be applied to predict the labels that were present in the training dataset. In real-life data, the vast majority of motion is unconstrained and can easily be misclassified by such models. Therefore, novel methods for building and evaluating robust and practical HAR models are needed.

One step in this direction is the work by [Willets et al., 2018], and associated open-sourced Capture24 dataset which contains 24h of real-world data from $N = 154$ research participants, alongside labels annotated using a body-worn video camera as ground truth. Using a combination of manual feature engineering, tree ensembles and temporal HMMs, they are able to build an accurate ($\kappa = 0.81$) 6-class HAR model.

1.3 Self-supervised HAR models

In recent years, self-supervised learning has gained significant attention due to its ability to learn without explicit labels. It involves a pre-training step where a proxy task is defined using information from the data itself. The output of the pre-training step is an encoder which transforms input data into features which are predictive of the proxy task. These features can be used by a new, usually much smaller, model which can be trained or fine-tuned on a labeled dataset to predict a downstream task of interest. Experiments in the field of image classification have shown Chen et al. [2020a], He et al. [2020], Chen et al. [2020b] that self-supervised models that have been pre-trained on large unlabeled datasets and fine-tuned on small labeled datasets can match or improve upon fully supervised models which need orders of magnitude more labeled data. This is valuable because, in contrast with labeled data, unlabeled data is usually cheap and abundant. There is also evidence that self-supervised models can be more robust and generalize better to new datasets [Hendrycks et al., 2019] than fully supervised models.

Recent attempts to apply self-supervised representation learning to the context of sensor-based Human Activity Recognition have by-and-large focused on demonstrating the generalizability of the *representation itself* by allowing the final few layers of the model to be learned directly on the dataset of interest, often the same small-scale or in-clinic datasets described above [Haresamudram et al., 2021, 2022, Saeed et al., 2019]. By testing the models in this way, they typically focus on label

efficiency, as a way to assess the representation quality: if the representation is rich enough, the final layers of the model can be trained using few labeled examples.²

This approach highlights that self-supervised learned representation are a viable alternative to hand-crafted engineered features as the basis for HAR models. It does not however, address the issue of the end-to-end model generalization to real-world settings.

These past efforts on self-supervised HAR have tried many combinations of optimization objectives, datasets and model architectures for both the pre-training and fine-tuning. Common optimization objectives include enforcing representation invariance across time, augmentations [Haresamudram et al., 2021, 2022, Saeed et al., 2019]. Common encoder architectures used include CNNs, RNNs, transformers. Linear or logistic regression models are used for evaluating representation quality while multiple dense layers are often used to make high performance end-to-end models. In Saeed et al. [2019], data augmentations are applied on IMU data and a self-supervised is trained to predict the transformation. Haresamudram et al. [2022] present an excellent analysis of auto-regressive models and transformers used to learn a representation of the IMU data that can predict neighbouring or future IMU data points, thus capturing the temporal characteristics of the signal. In this work, we combine temporal and transformation constraints to train a robust self-supervised encoder.

Concurrent with this work, Yuan et al. [2022] obtained good results using self-supervised representation as the basis for an HAR model, and evaluate it on the Capture24 dataset ($\kappa = 0.726$). Although performance is lower than previously published (fully supervised) models on that dataset, this is a promising step towards building a real-world HAR model using self-supervised learning.

1.4 Main contributions

This work builds on these past efforts and provides three novel contributions:

- First, we show *out-of-distribution generalization* $\kappa = 0.7$ of our end-to-end HAR model (including the self-supervised representation) by using the real-world labeled Capture24 dataset for *model evaluation only*. We think that this model evaluation framework is closest to how HAR algorithms are actually used: in real-world settings, and on devices different from the one used for training.
- Second, we leverage the self-supervised representations to combine disparate datasets using different sensors: the public in-clinic PAMAP2, together with an internal real-world dataset where labels are obtained from participant-reported tags. Further, we show that the performance of the final model largely improves upon that of models trained on the underlying separate datasets. This shows that the self-supervised representations can provide a natural standardization layer and can help reduce the data fragmentation in the field.
- Finally, we establish new state-of-the-art performance ($\kappa = 0.86$) for 6-class Human Activity Recognition on the Capture24 free-living video-labeled dataset. This shows that self-supervised pretraining is advantageous even when it is done on a different device.

2 Methods

2.1 Datasets

2.1.1 Benchmark HAR datasets

We used 4 public datasets incorporating labeled activities of daily living: PAMAP2 [Reiss and Stricker, 2012], Capture24 [Willettts et al., 2018], MHealth and Daily Sports. PAMAP2 contains data of 9 of participants who perform a predetermined set of activities, along with the start and end time of each activity. PAMAP2, MHealth and Daily Sports contain IMU data measured from wrist-worn devices and are available at the UCI Machine Learning Repository <http://archive.ics.uci.edu/ml/index.php>. Capture 24 contains data from 154 participants, followed over 24 hours of unscripted daily living. In

²An important clarification should be made for self-supervised encoder models that are pre-trained on unlabeled datasets and fine-tuned on labeled datasets. Since neural networks can easily memorize small datasets, such evaluations should not be considered evidence for generalization. Thus in this work, we evaluate our frozen pre-trained representation across multiple datasets and our end-to-end trained model on an entirely new dataset.

addition to the wrist-worn accelerometer, participants wear a body-worn camera which is used by human annotators to generate the activity labels. Table 1 summarizes the metadata of the benchmark datasets.

Dataset	#labeled classes	N	Device (sampling rate)	Location	Context
MHealth	12	10	Shimmer2 (50 Hz)	right wrist	scripted
PAMAP2	18	9	Colibri (100Hz)	dominant wrist	scripted
DailySports	19	8	Xsens MTx (25Hz)	left, right wrist	scripted
Capture24	6	154	Axivity AX3 (100Hz)	dominant wrist	real-world
Internal Pilot	8	85	Verily Study Watch (30Hz)	randomized	real-world

Table 1: Summary of benchmark datasets metadata.

2.1.2 Project Baseline Health Study

The self-supervised model was pre-trained using a 1-month period of free-living data collected in the Project Baseline Health Study (PBHS) [Arges et al., 2020] via a smartwatch (Verily Study Watch) equipped with an accelerometer.

The Project Baseline Health Study is a prospective, multi-center, longitudinal study that aims to map human health through a comprehensive understanding of the health of an individual and how it relates to the broader population. As part of the PBHS, participants agree to wear a wrist-worn device during daily activities that continuously collects high-resolution IMU data. In our study, we used these data to create a representation of activity without any labels.

No filtering or inclusion/exclusion criteria were applied beyond those of the main PBHS study, yielding 42,000 hours (≈ 15 million 10s windows) of accelerometer data from approximately 1200 study participants. During model training, no labels of activity or health were used and the only context used to identify accelerometer data was the device identifier and timestamp.

2.1.3 Free-living internal Pilot dataset

A total of 85 participants were asked to wear the Verily Study Watch over a one to two week period. They were able to self-report activities as they occurred throughout their daily living by tagging start and end times directly on the watch. Half of the participants were randomly picked and asked to wear the watch on the right hand and the other half were asked to wear it on the left hand. Participants were instructed to use the firmware on the watch to tag when they were starting an activity and end the tag when they ended the activity. Participants were not asked to record every instance of every activity, but to voluntarily tag as many as possible. We received over 1000 hours of tagged data in 5 activity classes as detailed in Table 2.

Later, a separate data collection effort was conducted, asking participants to tag the time when they went to bed with the intent of sleeping. In order to more precisely capture sleep epochs, the first and last 15 minutes of each tagged epoch were removed from the final dataset.

Activity	#hours	#unique participants
Exercise	61	47
Sedentary (Sit/Stand)	420	80
In motor vehicle	175	69
Walk/Run	45	36
Household chores	134	73
Sleep / in-bed	196	13

Table 2: Distribution of activities in pilot dataset.

2.2 Data preprocessing

Since the datasets we used have data from different devices and different sampling rates, we first standardized input data by normalizing all values to units of G ($9.8m/s^2$) and resampled all time

series to a regular time-grid at 30Hz. Resampling with and without anti-aliasing did not result in any notable difference in performance. A literature survey shows that most activities of daily living are captured under a frequency limit of 5 Hz, therefore a sampling rate of 30Hz is above the Nyquist frequency and aliasing should not be a concern. Next, we divided the time series into non-overlapping windows of 10 seconds each.

Each window contains 3 time series corresponding to x , y and z components of IMU identified by the device identifier and the starting timestamp of the window. Although the various devices are not always guaranteed to have the x , y and z channels map to the same axes in the watch reference frame, we did not standardize them prior to training. Because of natural variations of watch wear on the left or right wrist, along with rotations around the wrists, these x , y and z channels cannot be assumed to be fixed in wrist-frame even for a given device type. Therefore, we elected to handle these sources of variability through data augmentations directly when training the representation model.

2.3 Self-supervision labels

We use a contrastive approach based on temporal coincidence for self-supervised learning. The principle is to learn a mapping from input (in this case, windows of accelerometer data) to an embedding vector space in which coincident pairs are closer to each other than pairs which are not coincident. Thus the choice of coincidence criteria decides the geometrical relationship between points in the embedding space. In this work, 2 main types of coincidence were used:

1. *Temporal proximity*: two windows were considered as coincident if they belong to the same user and occur within a specified time Δt . The temporal proximity criterion creates clusters of ‘slow-moving’ activities (i.e. activities that have the same underlying structure over periods as long as or longer than Δt). For this study, we chose a maximum temporal proximity distance $\Delta t = 60$ seconds.
2. *Augmentation*: a transformation was applied on the accelerometer signal and the original and augmented views were considered coincident. This criterion makes the representation invariant to certain perturbations that resemble common forms of noise, or variations seen within and between accelerometers. For example, we added random jump in baselines, baseline wander, median filtering, rotation in the x - y plane and Gaussian noise. For each of these augmentations and their compositions, we made pairs using the original window and its augmented version. Figure 1 shows the transformations we used, along with examples of their effect on the data.

The construction of the optimization objective was inspired by the recent work in images and audio [Jansen et al., 2019, Ren et al., 2015]. Coincident pairs are created before training by sampling data from the full dataset and applying the constraints described above. Thus the input to the encoder with a batch size of b contains b pairs of IMU windows where each pair is randomly sampled from the dataset.

Figure 2 depicts how negative pairs were created during training, we simply consider all the possible pairs that can be constructed by $2b$ IMU windows: $4b^2$. There are b (*2 permutations) pairs with positive labels; these were the coincident pairs created in the previous step. We have an additional $2b$ identity pairs (pairs of the window with itself). The remaining $4b^2 - 4b$ pairs are combinations of windows which are randomly sampled from the dataset and can be considered unrelated pairs and thus labeled negative. This is a valid approximation that holds for large datasets where the number of subjects $> b$ and the number of windows per subject $>> b$. Since there were many more negative pairs than positive, we down-weighted negative labels by a factor of $(2b - 2)$ and down-weighted the identity pairs to 0.

2.4 Pre-training

The encoder ‘encodes’ a given 10-second window of 3-axis accelerometer data into a 256-dimensional feature vector. The encoder architecture of the model is a convolutional tower with c convolutional blocks, followed by a dense layer with d -dimensional embedding output. We experimented with various hyperparameters and achieved stable results with $c = 5$ convolutional blocks and the $d = 256$ embedding size.

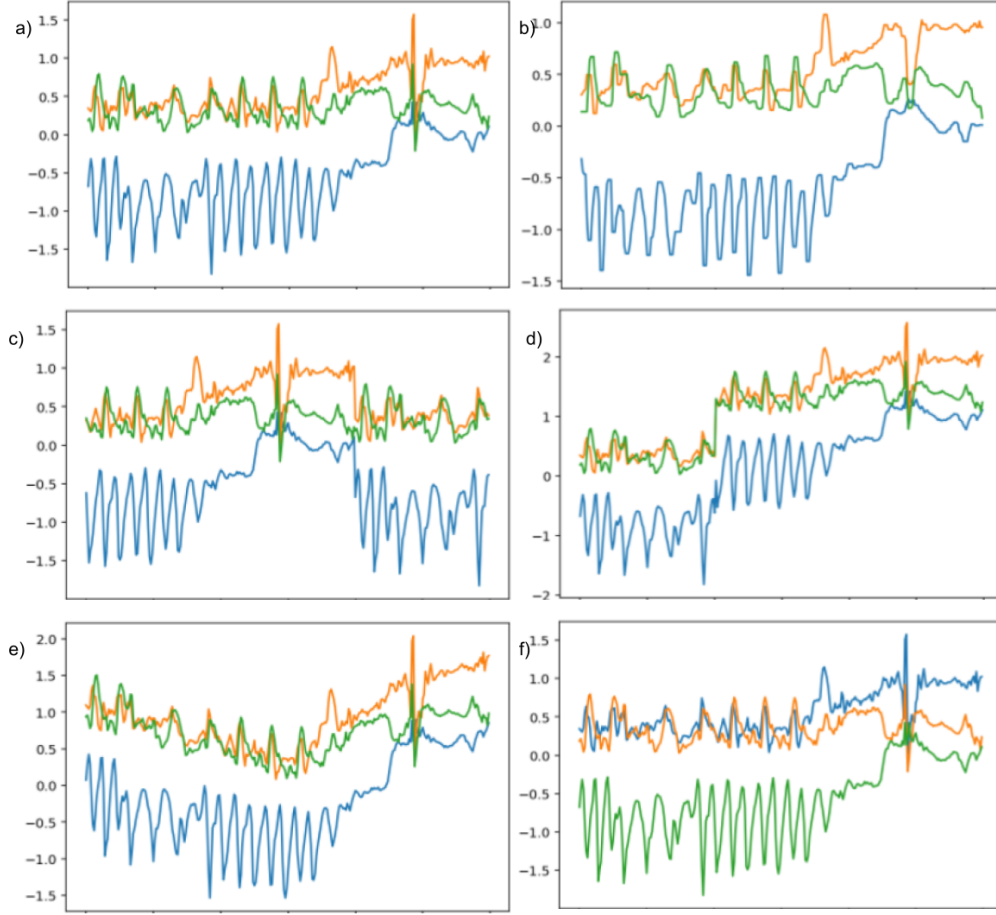


Figure 1: Augmentations. a) is the original window and the rest are its augmented versions. b) is the smoothed window, c) has been translated in time, d) has a discontinuous jump in the baseline, e) has a gradual baseline wander, and f) is rotated in 3-axis.

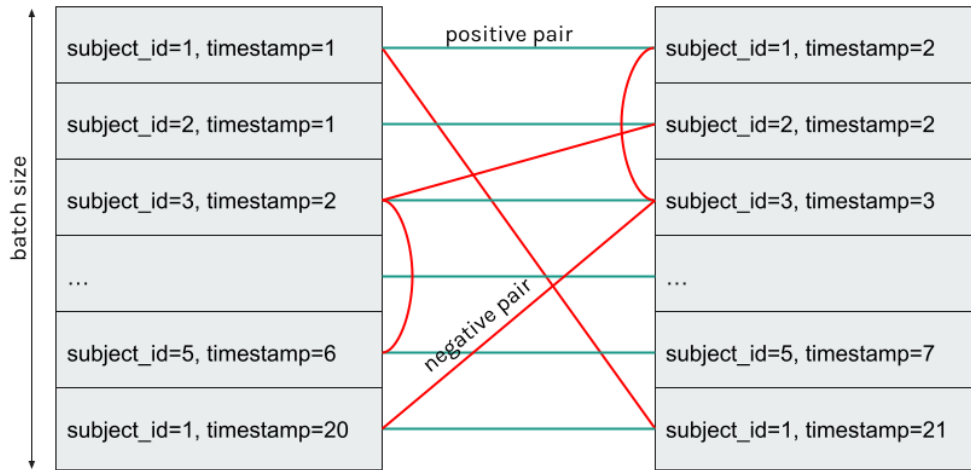


Figure 2: Pair labeling network: Training inputs are batches of paired windows. Pairs ii (connected by green lines) for i^{th} element of the batch are positive pairs that were sampled before training. Pairs ij (connected by red lines) for $i \neq j$ are random combinations. For a large shuffled dataset, these combinations can be assumed to be negative pairs.

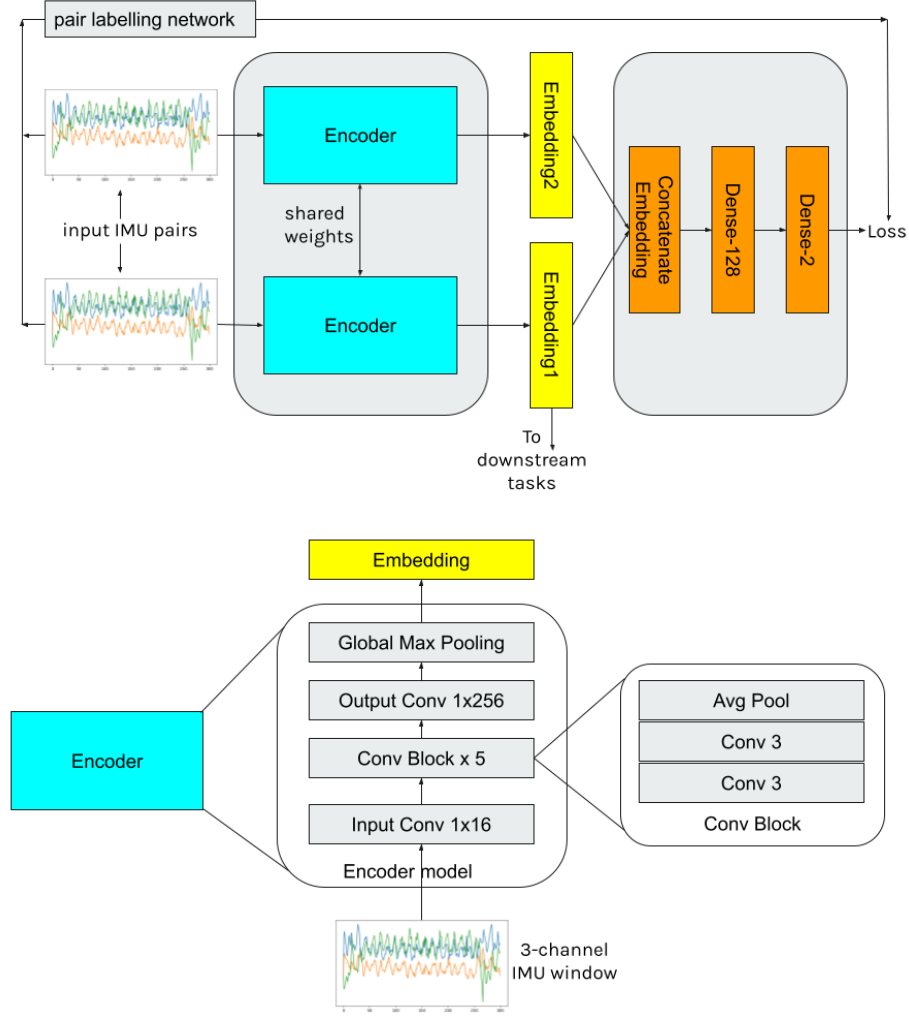


Figure 3: Model training pipeline. The main model is the convolutional neural network encoder which takes 10 second accelerometer windows as input and returns a vector embedding. The auxiliary dense layers are added during training to predict which pairs of IMU windows are labeled as positive.

During training, coincident pairs are picked randomly from the dataset, stacked in batch dimension and fed to the encoder to get embeddings for all windows (i.e., if the original batch size is $b = 128$, effective batch size to encoder is $2 * b = 256$). We then created paired embeddings by concatenating the embeddings of all possible pairs of windows in the batch (i.e. $(2 * b) * (2 * b) = 65,536$ paired embeddings). The resulting paired embeddings were then fed into a 2-layer perceptron projector. The output of the perceptron is a binary softmax prediction, with negative or class 0 indicating the two windows are not coincident and positive or class 1 indicating that the two windows are coincident. The corresponding positive and negative labels are created as described above. The training loss was a cross-entropy loss between the predicted binary prediction and the coincidence labels. This loss - which uses only the IMU windows and the device and timestamp identifiers of the windows and no external oracle and thus *self-supervised* - cause the encoder to extract features that are invariant to noise and can characterize motion that is consistent over time. Training was performed for 0.5 million steps and the model was then saved.

During inference, we drop the loss network, and the encoder takes as input a single 10-second window and returns a 256-element feature vector or embedding. Figure 3 shows the architecture of the full training pipeline, specifically the encoder model.

2.5 Training the final HAR head

Some of the evaluation datasets may have severe class imbalance. This is especially the case for the ones where data is collected in the real world, and where class balances are reflective of the natural occurrence of various activities. In order to avoid class collapse when training with categorical cross-entropy, we re-weight the minority class to be no less than 5x smaller than the majority class. During evaluation, the original class balance is used.

Our model is a simple fully-connected perceptron with 5 layers and 128 neurons each. At inference time, class prediction logits are smoothed temporally over a 2-minute window. We find that this temporal smoothing mechanism increases classification accuracy.

2.6 Benchmark

In order to better understand the benefit of self-supervision, we provide performance when a simplified HAR head (1-layer perceptron) is trained using only 8 first and second-order statistics of the 10s signal: the means and std of the acceleration along the xyz axes, and the mean and standard deviation of the vector norm of the acceleration. We find that these features, termed *benchmark* yields surprisingly strong results which outperform some of the existing published results on our datasets of interest.

3 Results

3.1 Accuracy of self-supervised representations

Similar to previous work, we first evaluate the usefulness of the representation model by training a simple linear classification model on top of the frozen representations. In Table 3, we show that our representations are useful for human activity recognition, leading to strong classification accuracy³, and can work across multiple sensors and datasets.

Authors (year)	PAMAP2	MHealth	DailySports
J. Wang et. al (2018)	39.21	-	57.97
Xin Qin et al (2020)**	63.9	-	60.7
Holzemann et al (2020)	20.1	-	-
TransAct (2017) **	-	82	85
Ours (benchmark)	74.3	82.4	72.8
Ours (self-supervised)	83.3	93.4	91.1

Table 3: Random test set activity classification accuracies achieved by comparable efforts that show generalization of models. ** indicates the performance is measured on a smaller set of activities than what is found in the dataset.

When evaluating models on real-world datasets such as Capture24, class imbalance can become a primary concern. As a result, previous works often report on κ scores rather than raw accuracy. In Table 4, we provide these numbers for the Capture24 dataset.

Authors (year)	Capture 24
Willetts et al. [2018]	.81
Yuan et al. [2022]	.726
Ours (self-supervised) [2023]	.86

Table 4: κ scores for comparable efforts at building general models

³Because we focus on generalization beyond any single dataset, here we provide comparisons only with previous work where model performance is provided for at least two distinct datasets.

3.2 Out-of-distribution generalization

To test the out-of-distribution generalization of our framework, we train 4 models on top of the self-supervised frozen representations, where the final classification head are trained respectively on Capture24, Pilot and the combination of PAMAP2 and Pilot. The lack of standardization of label semantics across datasets poses a key challenge arises when attempting to evaluate out-of-distribution generalization for an HAR model. Table 5 shows how the classes of the PAMAP2 and Pilot datasets map to the classes in Capture24. Although we take special care when mapping the class semantics of one dataset to those of another, some semantic differences remain, and likely account for some of the lower out-of-distribution performance compared to in-distribution.

Capture24 class	PAMAP2 classes	Pilot classes
Sleep	-	sleep / in-bed
sit-stand	stand	standing in place still
	sit	
	computer	
	lying TV	
vehicle	drive	in motor vehicle
walking	walk	slow walking Walk-run
	run	
	desc stairs	
	nordic_walk asc stairs	
mixed activity	clean house	household chores
	fold_laundry	
	iron	
	rope_jump	
	soccer vacuum	
bicycling	cycling	sports

Table 5: Model performance when varying the data used for training the final HAR head. * indicates that the training and evaluation datasets are different, indicating out-of-distribution setup.

In Table 6, we provide the out-of-distribution generalization of various models where the final training is performed on either Capture24, PAMAP2 or the Pilot dataset.

Training data	metric	Eval: Capture24	Eval: Pilot
Capture24	κ	.86	.66*
Pilot dataset	κ	.54*	.72
Pilot dataset + PAMAP2	κ	.70*	.71

Table 6: Model performance when varying the data used for training the final HAR head. * indicates that the training and evaluation datasets are different, indicating out-of-distribution setup.

In particular, we observe that the model trained on the combined Pilot + PAMAP2 dataset has similar out-of-distribution performance (on Capture24) and in-distribution (on the Pilot data), indicating good generalization performance.

In Figure 4, we observe the sources of misclassification for both the in-distribution Capture model, as well as our best combined model.

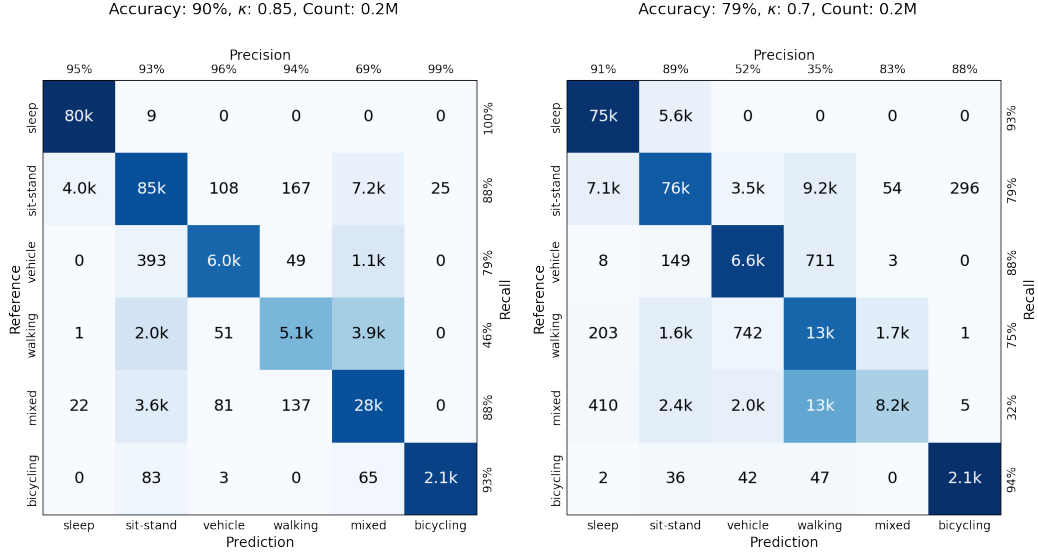


Figure 4: Confusion matrices for on the Capture24 dataset. Left is the model trained on Capture24 (in-distribution). Right is the model trained on PAMAP2 + Pilot datasets (out-of-distribution).

4 Discussion

Our work combines some of the documented attributes of previous efforts in HAR, such as self-supervised representations, data augmentations and temporal proximity pairs, and combine that with a large pre-training dataset. We demonstrate the power of using a large unlabeled training dataset to pre-train powerful self-supervised representations of human motion. We show that training a CNN on a large dataset can produce state of the art results and show excellent generalization to new datasets and new devices. Using both the temporal proximity and data augmentation loss provide sufficient context for our model to learn highly discriminative features representations. We demonstrate that the learned representation can extract highly discriminative features which can be used to recognize human activity.

Therefore in a practical application, we believe the essential first-order component of a robust HAR system is a robust feature representation that can generalize to new devices and subjects.

Finally, we summarize the considerations we implement to ensure evaluation and comparison of HAR models. In particular, we note that our benchmark evaluation shows that even trivial statistical features can easily show very strong performance within a single dataset, therefore it is a useful method to assess the value of complex models and the ease of separability of different datasets. The benchmark models also fail when trained on one dataset and applied on a new dataset, highlighting the importance of testing cross-dataset generalization.

4.1 Limitations and future work

There are a few limitations of our proposed HAR framework. First, the training objective of our self-supervised loss assumes that temporally adjacent windows are likely to be part of the same activity. This objective enables the encoder to learn a rich representation for ‘slow-moving’ activities (i.e. activities that have the same underlying structure for at least 1-5 minutes). However, this objective could potentially act against learning rich representations of activities that last less than 1 minute (e.g. standing up from a chair or opening doors). The second training objective, which uses augmentations instead of temporal proximity for defining coincidence pairs, is better suited to represent these activities. More analysis is needed to quantify the impact of the 2 objectives and how they affect different activities. This will require more detailed studies with many more activities than are found in the benchmark datasets.

Our design choice of providing classification at the 10 second level fundamentally limits the time scale at which representations are learned. As a result, this limits the model’s ability to recognise more complex activities which may occur at the 5-30 minute time scale. Further work with longer time windows could lead to improvements, and reduce the need for our own approach of using temporal smoothing to increase model robustness.

Acknowledgments and Disclosure of Funding

We thank Erin Rainaldi, Ritu Kapur, Anthony Chan, David Andresen and Stephen Lanham for the organization, collection and compilation of the free-living pilot dataset with the Verily Study Watch. We thank Aren Jansen for invaluable guidance and feedback in designing the concept and implementation of self-supervised machine learning models. We thank Sara Popham for critical feedback and analysis of the model. We thank the UCI Machine learning dataset repository, Mohammad Malekzadeh, and USC for hosting the public benchmark datasets used in this effort. We thank all the participants in the Project Baseline Health Study and the pilot study for their participation.

Verily Life Sciences, LLC, funded the work and the research studies. All authors were full time employees of Verily Life Sciences during their contributions to this effort. No financial compensation was received outside of the contributors’ regular monetary and stock compensation due to their employment at Verily Life Sciences.

References

- Kerem Altun, Billur Barshan, and Orkun Tunçel. Comparative study on classifying human activities with miniature inertial and magnetic sensors. *Pattern Recognition*, 43(10):3605–3620, 2010. ISSN 0031-3203. doi: <https://doi.org/10.1016/j.patcog.2010.04.019>. URL <https://www.sciencedirect.com/science/article/pii/S0031320310001950>.
- Kristine Arges, Themistocles Assimes, Vikram Bajaj, Suresh Balu, Mustafa R Bashir, Laura Beskow, Rosalia Blanco, Robert Califf, Paul Campbell, Larry Carin, et al. The project baseline health study: a step towards a broader mission to map human health. *NPJ digital medicine*, 3(1):1–10, 2020.
- No authors listed. The Unified Parkinson’s Disease Rating Scale (UPDRS): status and recommendations. *Mov Disord*, 18(7):738–750, Jul 2003.
- O. Banos, C. Villalonga, R. Garcia, A. Saez, M. Damas, J. A. Holgado-Terriza, S. Lee, H. Pomares, and I. Rojas. Design, implementation and validation of a novel open framework for agile development of mobile health applications. *Biomed Eng Online*, 14 Suppl 2:S6, 2015.
- Barbara Bruno, Fulvio Mastrogiovanni, Antonio Sgorbissa, Tullio Vernazza, and Renato Zaccaria. Analysis of human behavior recognition algorithms based on acceleration data. In *2013 IEEE International Conference on Robotics and Automation*, pages 1602–1607, 2013. doi: 10.1109/ICRA.2013.6630784.
- Ting Chen, Simon Kornblith, Mohammad Norouzi, and Geoffrey Hinton. A simple framework for contrastive learning of visual representations. In *International conference on machine learning*, pages 1597–1607. PMLR, 2020a.
- Xinlei Chen, Haoqi Fan, Ross Girshick, and Kaiming He. Improved baselines with momentum contrastive learning. *arXiv preprint arXiv:2003.04297*, 2020b.
- M. A. Clynes, K. A. Jameson, M. H. Edwards, C. Cooper, and E. M. Dennison. Impact of osteoarthritis on activities of daily living: does joint site matter? *Aging Clin Exp Res*, 31(8):1049–1056, Aug 2019.
- J. de Rotrou, Y. H. Wu, L. Hugonot-Diener, C. Thomas-Antérion, J. S. Vidal, M. Plichart, A. S. Rigaud, and O. Hanon. DAD-6: A 6-item version of the Disability Assessment for Dementia scale which may differentiate Alzheimer’s disease and mild cognitive impairment from controls. *Dement Geriatr Cogn Disord*, 33(2-3):210–218, 2012.

- E. B. Fauth, S. Schwartz, J. T. Tschanz, T. Østbye, C. Corcoran, and M. C. Norton. Baseline disability in activities of daily living predicts dementia risk even after controlling for baseline global cognitive ability and depressive symptoms. *Int J Geriatr Psychiatry*, 28(6):597–606, Jun 2013.
- Harish Haresamudram, Irfan Essa, and Thomas Plotz. Contrastive predictive coding for human activity recognition. *Proc. ACM Interact. Mob. Wearable Ubiquitous Technol.*, 5(2), jun 2021. doi: 10.1145/3463506. URL <https://doi.org/10.1145/3463506>.
- Harish Haresamudram, Irfan Essa, and Thomas Plötz. Assessing the state of self-supervised human activity recognition using wearables, 2022. URL <https://arxiv.org/abs/2202.12938>.
- Kaiming He, Haoqi Fan, Yuxin Wu, Saining Xie, and Ross Girshick. Momentum contrast for unsupervised visual representation learning. In *Proceedings of the IEEE/CVF conference on computer vision and pattern recognition*, pages 9729–9738, 2020.
- Dan Hendrycks, Mantas Mazeika, Saurav Kadavath, and Dawn Song. Using self-supervised learning can improve model robustness and uncertainty. *CoRR*, abs/1906.12340, 2019. URL <http://arxiv.org/abs/1906.12340>.
- Aren Jansen, Daniel P. W. Ellis, Shawn Hershey, R. Channing Moore, Manoj Plakal, Ashok C. Popat, and Rif A. Saurous. Coincidence, categorization, and consolidation: Learning to recognize sounds with minimal supervision. *CoRR*, abs/1911.05894, 2019. URL <http://arxiv.org/abs/1911.05894>.
- M. Kazama, N. Kondo, K. Suzuki, J. Minai, H. Imai, and Z. Yamagata. Early impact of depression symptoms on the decline in activities of daily living among older Japanese: Y-HALE cohort study. *Environ Health Prev Med*, 16(3):196–201, May 2011.
- K. Kroenke, R. L. Spitzer, and J. B. Williams. The PHQ-9: validity of a brief depression severity measure. *J Gen Intern Med*, 16(9):606–613, Sep 2001.
- Benjamin Lam, Michael Catt, Sophie Cassidy, Jaume Bacardit, Philip Darke, Sam Butterfield, Ossama Alshabrawy, Michael Trenell, Paolo Missier, et al. Using wearable activity trackers to predict type 2 diabetes: machine learning-based cross-sectional study of the uk biobank accelerometer cohort. *JMIR diabetes*, 6(1):e23364, 2021.
- B. J. Lawrence, N. Gasson, R. Kane, R. S. Bucks, and A. M. Loftus. Activities of daily living, depression, and quality of life in Parkinson’s disease. *PLoS One*, 9(7):e102294, 2014.
- Mohammad Malekzadeh, Richard G. Clegg, Andrea Cavallaro, and Hamed Haddadi. Protecting sensory data against sensitive inferences. In *Proceedings of the 1st Workshop on Privacy by Design in Distributed Systems, W-P2DS’18*, New York, NY, USA, 2018. Association for Computing Machinery. ISBN 9781450356541. doi: 10.1145/3195258.3195260. URL <https://doi.org/10.1145/3195258.3195260>.
- C. Marra, J. L. Chen, A. Coravos, and A. D. Stern. Quantifying the use of connected digital products in clinical research. *NPJ Digital Medicine*, 3:50, 2020.
- G. A. Marshall, R. E. Amariglio, R. A. Sperling, and D. M. Rentz. Activities of daily living: where do they fit in the diagnosis of Alzheimer’s disease? *Neurodegener Dis Manag*, 2(5):483–491, Oct 2012.
- Attila Reiss and Didier Stricker. Introducing a New Benchmarked Dataset for Activity Monitoring. *2012 16th International Symposium on Wearable Computers*, pages 108–109, 2012. doi: 10.1109/ISWC.2012.13.
- Shaoqing Ren, Kaiming He, Ross B. Girshick, and Jian Sun. Faster R-CNN: towards real-time object detection with region proposal networks. *CoRR*, abs/1506.01497, 2015. URL <http://arxiv.org/abs/1506.01497>.

- Aaqib Saeed, Tanir Ozcelebi, and Johan Lukkien. Multi-task self-supervised learning for human activity detection. *Proceedings of the ACM on Interactive, Mobile, Wearable and Ubiquitous Technologies*, 3(2):1–30, jun 2019. doi: 10.1145/3328932. URL <https://doi.org/10.1145/3328932>.
- O. Sandberg, K. A. Franklin, G. Bucht, and Y. Gustafson. Sleep apnea, delirium, depressed mood, cognition, and ADL ability after stroke. *J Am Geriatr Soc*, 49(4):391–397, Apr 2001.
- Catherine Tong, Shyam A. Tailor, and Nicholas D. Lane. Are accelerometers for activity recognition a dead-end? *CoRR*, abs/2001.08111, 2020. URL <https://arxiv.org/abs/2001.08111>.
- Michael Wainberg, Samuel E Jones, Lindsay Melhuish Beaupre, Sean L Hill, Daniel Felsky, Manuel A Rivas, Andrew SP Lim, Hanna M Ollila, and Shreejoy J Tripathy. Association of accelerometer-derived sleep measures with lifetime psychiatric diagnoses: A cross-sectional study of 89,205 participants from the uk biobank. *PLoS Medicine*, 18(10):e1003782, 2021.
- Matthew Willetts, Sven Hollowell, Louis Aslett, Chris Holmes, and Aiden Doherty. Statistical machine learning of sleep and physical activity phenotypes from sensor data in 96,220 uk biobank participants. *Scientific reports*, 8(1):1–10, 2018.
- James R. Williamson, Brian Telfer, Riley Mullany, and Karl E. Friedl. Detecting parkinson’s disease from wrist-worn accelerometry in the u.k. biobank. *Sensors*, 21(6), 2021. ISSN 1424-8220. doi: 10.3390/s21062047. URL <https://www.mdpi.com/1424-8220/21/6/2047>.
- Hang Yuan, Shing Chan, Andrew P Creagh, Catherine Tong, David A Clifton, and Aiden Doherty. Self-supervised learning for human activity recognition using 700,000 person-days of wearable data. *arXiv preprint arXiv:2206.02909*, 2022.
- Mi Zhang and Alexander A. Sawchuk. Usc-had: A daily activity dataset for ubiquitous activity recognition using wearable sensors. In *Proceedings of the 2012 ACM Conference on Ubiquitous Computing*, UbiComp ’12, page 1036–1043, New York, NY, USA, 2012. Association for Computing Machinery. ISBN 9781450312240. doi: 10.1145/2370216.2370438. URL <https://doi.org/10.1145/2370216.2370438>.